Supplementary information for

Investigation of different degradation pathways for organic photovoltaics at different temperatures

Bradley P. Kirk [1], Amira R. Alghamdi [1,2], Matthew J. Griffith [3,4], Xun Pan [1], Martyn Jevric [1], David A. Lewis [1], Gunther G. Andersson [1], Mats R. Andersson [1*]

[1] Flinders Institute for Nanoscale Science and Technology, College of Science and Engineering, Flinders University, P.O. Box 2100, Adelaide, SA 5001, Australia

[2] Department of Physics, College of Science, Imam Abdulrahman Bin Faisal University, P.O. Box 1982, Dammam 31441, Saudi Arabia

[3] Future Industries Institute, University of South Australia, Mawson Lakes, SA, 5095, Australia

[4] School of Aerospace, Mechanical and Mechatronic Engineering, University of Sydney, Camperdown, NSW, 2006, Australia

*Email: mats.andersson@flinders.edu.au

S.1. Zinc oxide nanoparticle synthesis

The ZnO nanoparticle (NP) dispersion ink was prepared based on a previously published procedure.[1] Zinc acetate dihyrdate (12 g, Sigma Aldrich) were dissolved in methanol (500 mL, Chem-supply, 99.9%) while potassium hydroxide (6 g, Chem-supply) were dissolved in methanol (250 mL , Chem-supply, 99.9%). Both solutions were heated up to 60 °C with virous stirring, prior to adding solutions together. The combined solution underwent gentle reflux for 4 hours. The solution was the allowed to sediment overnight before removing majority of the methanol via decanting. Acetone was added to the sediment until the concentration was approximately 35 - 40 mg mL^{-1}. 2-(2-methoxyethoxy) acetic acid (MEA) (6-8% W/W in relation to ZnO NP) (Sigma Aldrich) was then added to the solution and mixed overnight.

S.2. Slot-die theoretical thickness

To determine the theoretical thickness of the specific layers coated via slot-die coating, the following equations were employed for wet (Eq. S1) and dry films (Eq. S2):

$$d_{wet} = \frac{f}{S\,w} \qquad \textbf{Eq. S1}$$

$$d_{dry} = \frac{f\ \ c}{S\,w\rho} \qquad \textbf{Eq. S2}$$

Where d is the thickness (cm), f is the flow rate ($cm^3\ min^{-1}$), S is the drum rotation speed ($cm\ min^{-1}$), w is the meniscus guide width (cm), c is the solid content in the ink ($g\ cm^{-3}$) and ρ is the density of the dried material.[2, 3] The estimated material density polymer to be 1.0 g mL^{-1}, while the densities for $PC_{61}BM$ & C_{60} are 1.5 g mL^{-1} [4] and 1.68 g mL^{-1} [5] respectively. The material densities of $PC_{71}BM$ & C_{70} are similar to $PC_{61}BM$ & C_{60} respectively.

S.3. Dynamic mechanical thermal analysis

The blend solutions used were the same as the ones used for solar cell fabrication. The prepared samples were dried under high vacuum of approximately 6×10^{-7} torr overnight. The measurements were performed in a strain-controlled tension mode at a heating rate of 3 °C min^{-1} from −110 to 300 °C under a nitrogen atmosphere at a frequency of 1 Hz. Short-time (30 min) annealing of samples was done in the DMA instrument under a nitrogen atmosphere for 30 min. Whereas long-time (from 1 hour to 1 week) annealing of the sample was done on a hotplate under dark, nitrogen conditions. The storage modulus (E′), loss modulus (E”) and Tan δ were recorded as a function of temperature for each sample.

S.4. Exponential decay fitting

For determining the decay rate of the thermally aged devices at 85 °C and 120 °C, exponential curve with linear trendline were fitted to the experimental data. The trendline fitting was achieved with the following equation (Eq. S3):

$$PCE = A\exp(-k * Aging) + B \qquad \textbf{Eq. S3}$$

Where $Aging$ is in terms of days, while (k) is the decay rate of the exponential decay function. The fitting was achieved with Origin 2021b, by utilising an Levenberg Marquardt Iteration Algorithm. Fitting of trendlines with experimental data can be seen below for 85 °C (Fig. S1) and 120 °C (Fig. S2).

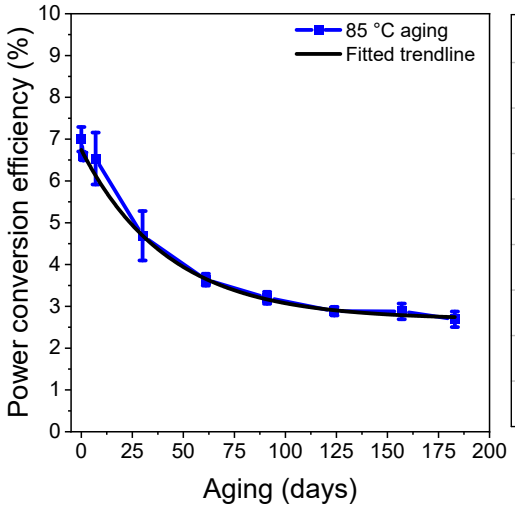

Model	ExpDec1
Equation	PCE = A*exp(-k*Aging) + B
Plot	Power conversion efficiency
B	2.68643 ± 0.07337
A	4.05736 ± 0.09235
k	0.02346 ± 0.00182
Reduced Chi-Sqr	0.2922
R-Square (COD)	0.99996
Adj. R-Square	0.99994

Fig. S1 Power conversion efficiency (PCE) changes as a function of ageing time for devices at 85 °C under dark nitrogen conditions, with fitted trendline (LEFT) and parameters related to trendline (RIGHT)

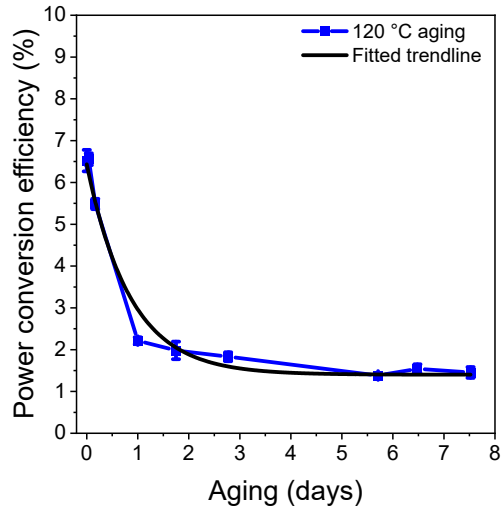

Model	ExpDec1
Equation	PCE = A*exp(-k*Aging) + B
Plot	Power conversion efficiency
B	1.40093 ± 0.0272
A	5.03301 ± 2.43862
k	1.17004 ± 0.38213
Reduced Chi-Sqr	0.50025
R-Square (COD)	0.9988
Adj. R-Square	0.9984

Fig. S2 Power conversion efficiency (PCE) changes as a function of ageing time for devices at 85 °C under dark nitrogen conditions, with fitted trendline (LEFT) and parameters related to trendline (RIGHT)

S.5. Extraction Under Reverse Bias vs Short Circuit

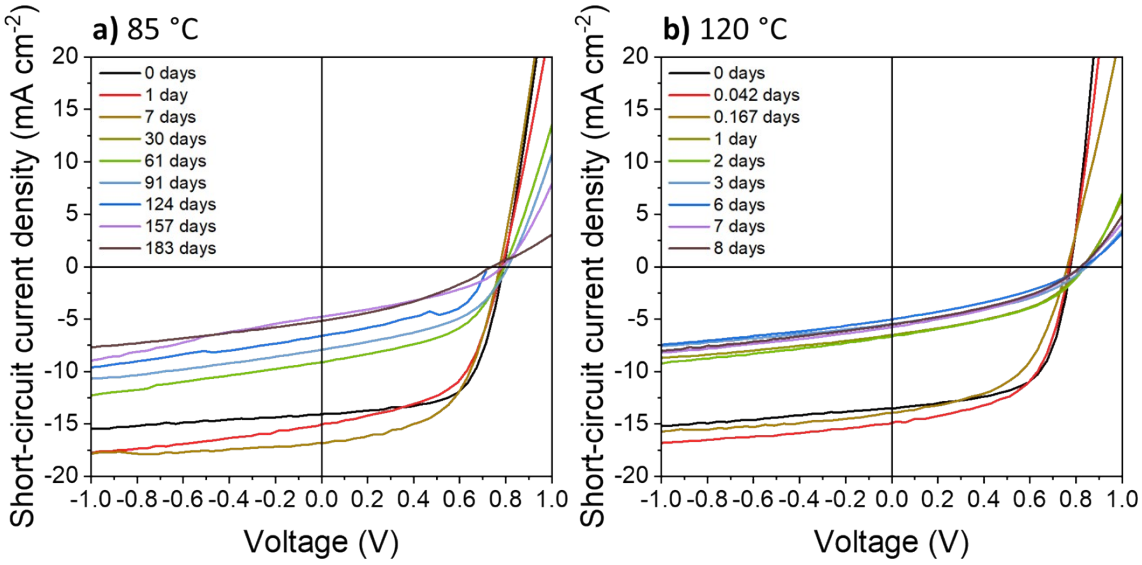

Fig. S3 J-V curves of cells that have either been aged at 85 °C (a) or 120 °C (b) under dark nitrogen conditions.

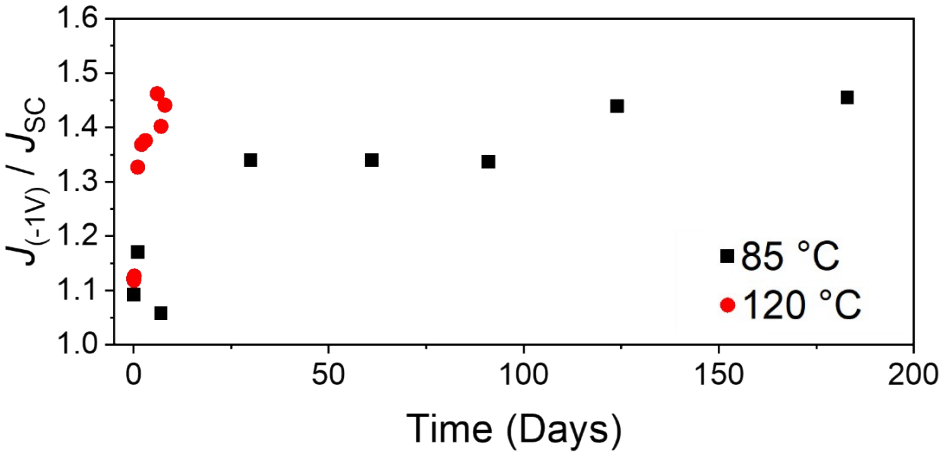

Fig. S4 Extraction Under Reverse Bias ($J_{(-1V)}$) vs Short Circuit (J_{SC}) in relation to ageing time. The values were extracted from the J-V curves in Fig. S3, with data sets separated into ageing temperatures (85 °C and 120 °C).

S.6. Charge carrier dynamics of inverted PPDT2FBT:$PC_{61}BM$ devices

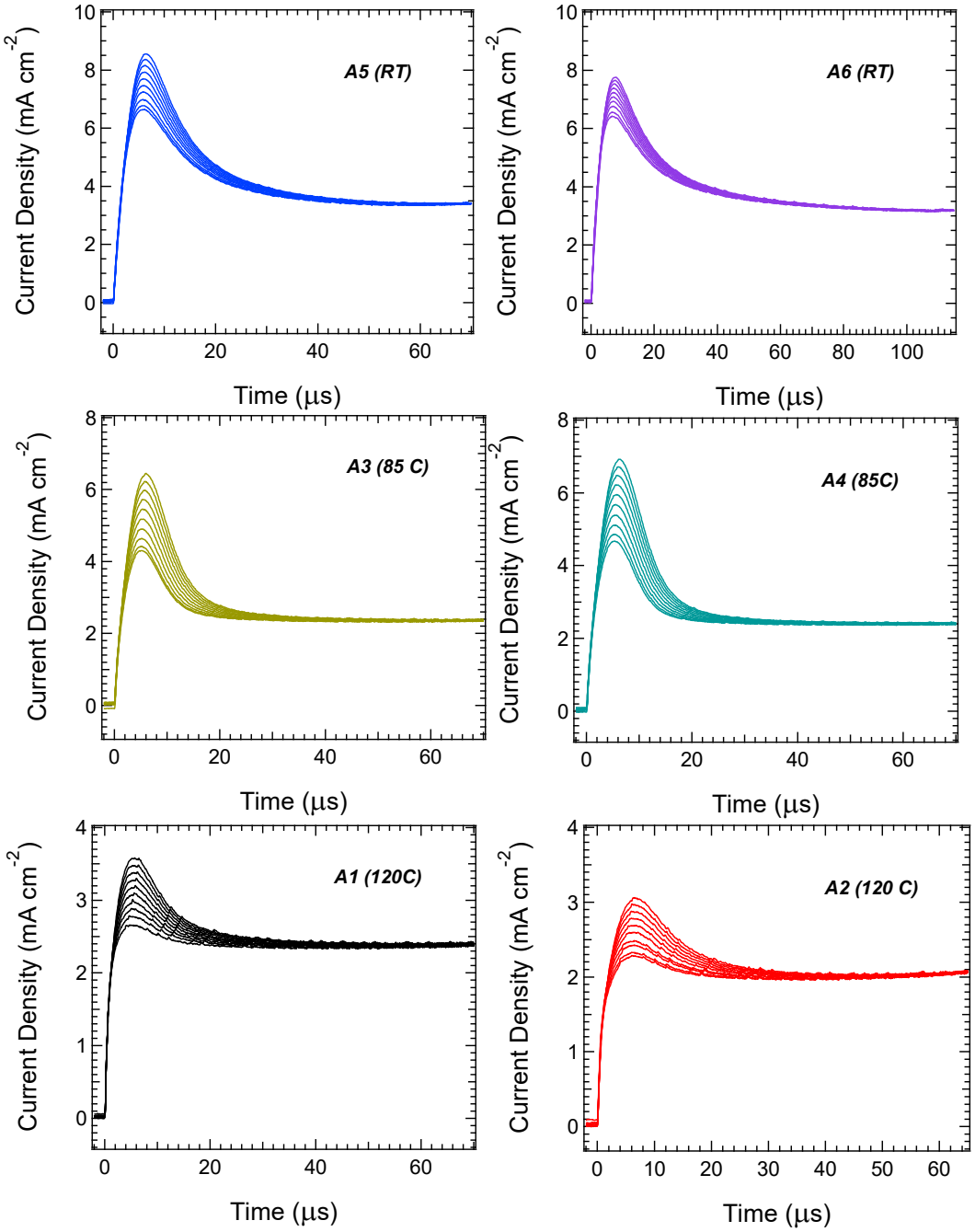

Fig. S5 photoCELIV results for inverted slot-die fabricated PPDT2FBT:$PC_{61}BM$ devices, thermally aged for 7 days at either room temperature (RT), 85 °C or 120 °C.

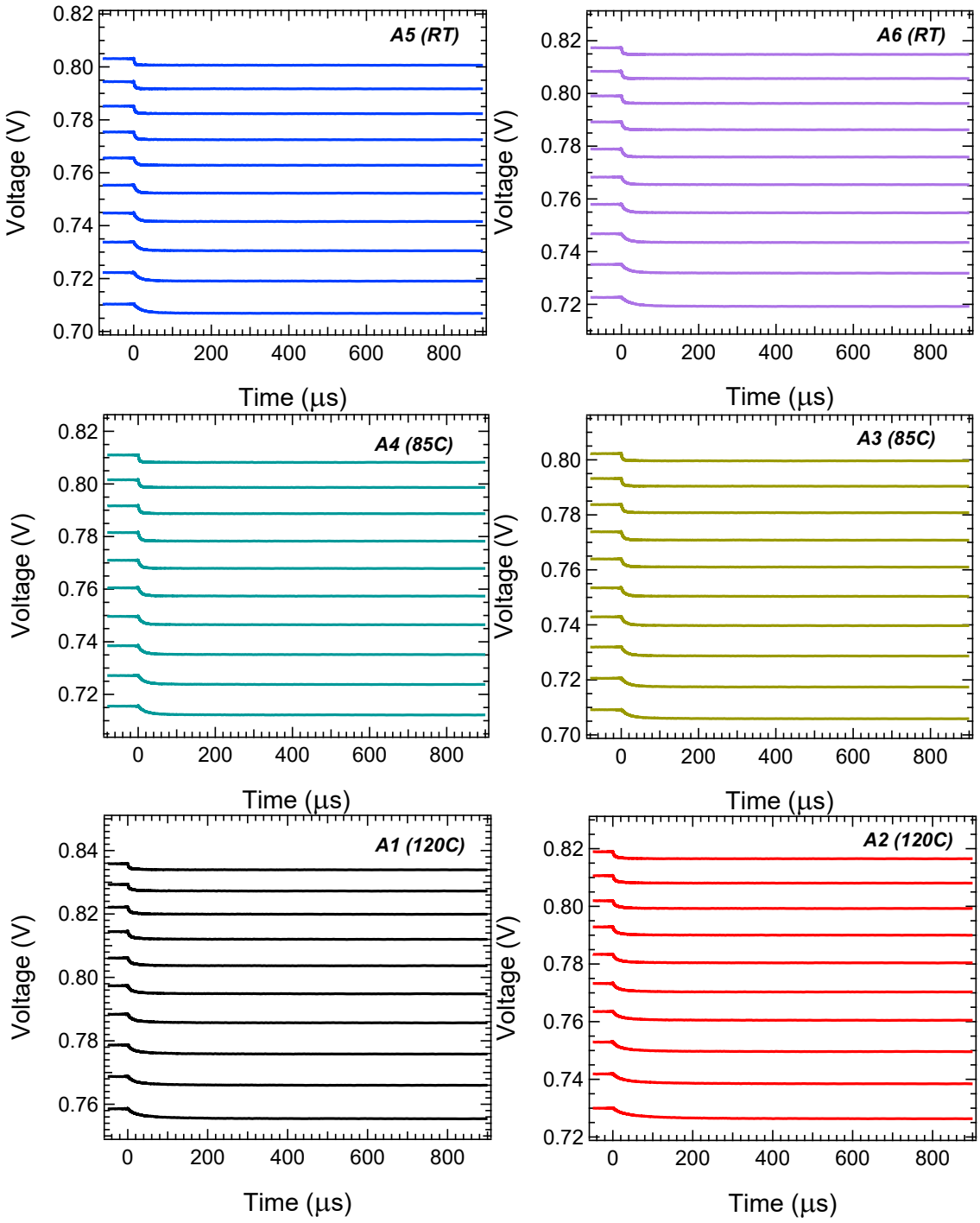

Fig. S6 TPV results for inverted slot-die fabricated PPDT2FBT:$PC_{61}BM$ devices, , thermally aged for 7 days at either room temperature (RT), 85 °C or 120 °C.

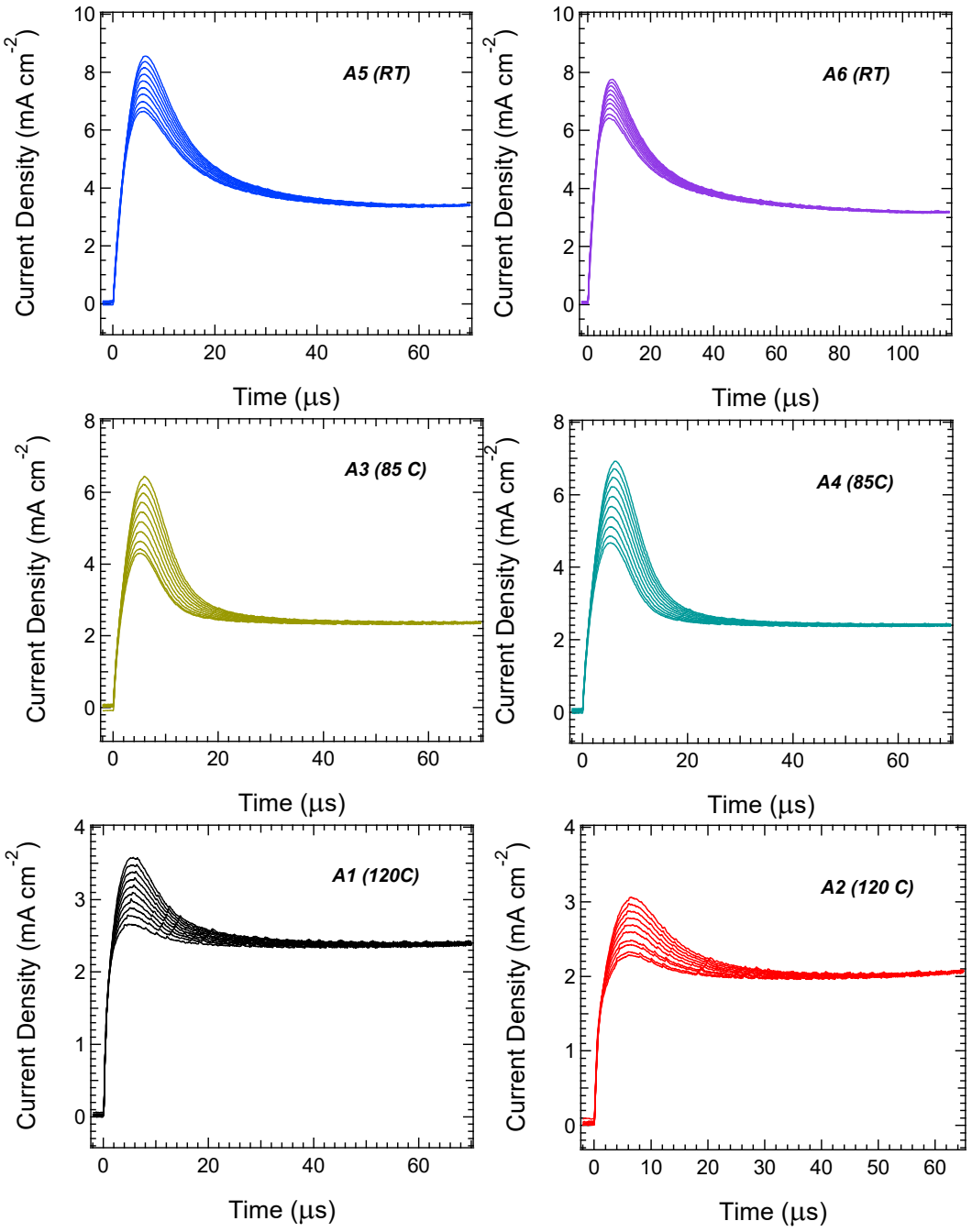

Fig. S7 TRCE results for inverted slot-die fabricated PPDT2FBT:$PC_{61}BM$ devices, thermally aged for 7 days at either room temperature (RT), 85 °C or 120 °C.

S.7. Comparing scanning electron spectroscopy images with stylus profilometry of 85 °C aged bulk heterojunction

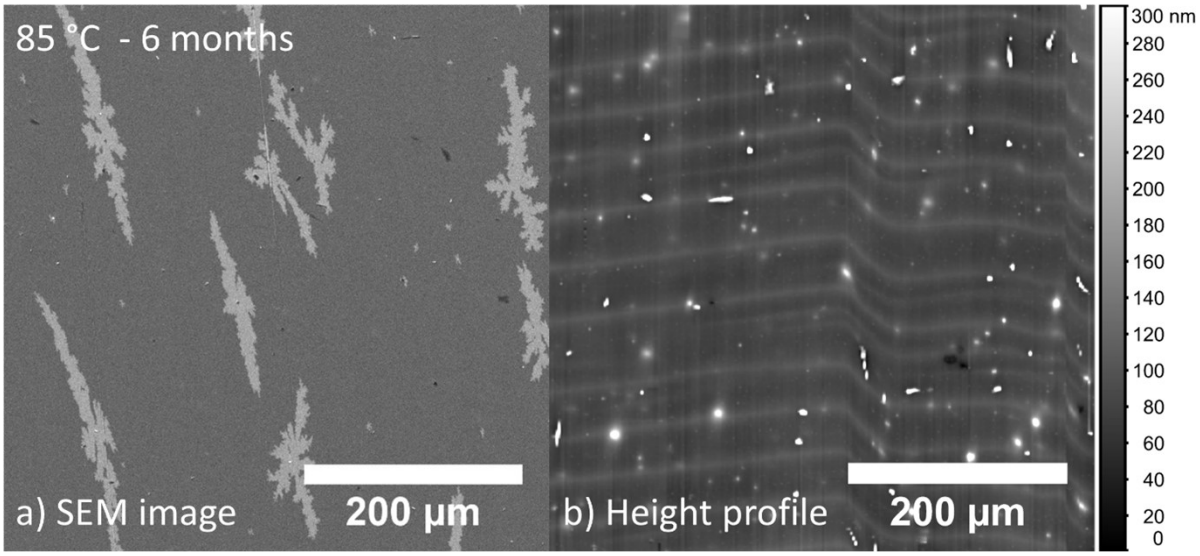

Fig. S8 Surface comparison of BHJ that was annealed at 85 °C for 6 months: a) SEM image, and b) Stylus Profilometry height image, with a z-scale bar (RIGHT).

S.8. Scanning electron microscopy images from Auger electron spectroscopy samples

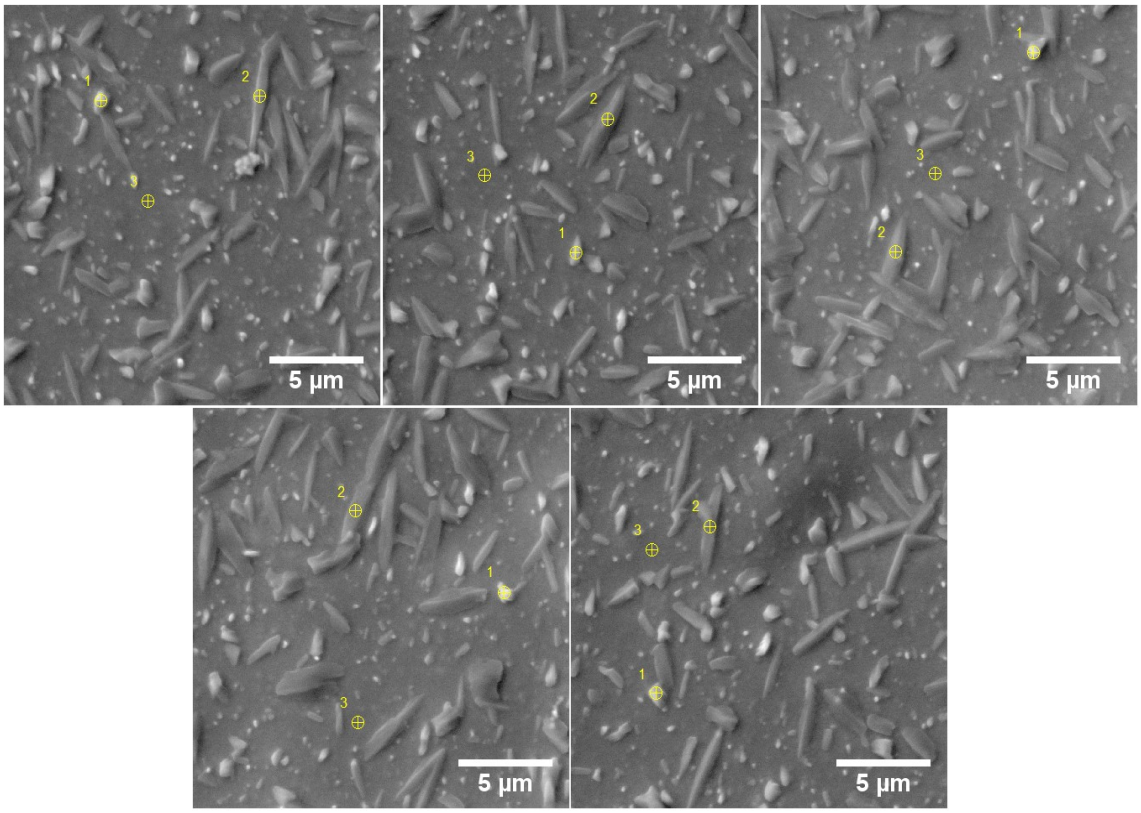

Fig. S9 SEM image of the PPDT2FBT:$PC_{61}BM$ surface after 8 hours at 120 °C with marked 0.65 µm diameter spot locations of Auger spectroscopy was measured. Position 1 & 2 is the spot scan location over the short and long crystals, respectively, while position 3 is over the surface of the BHJ.

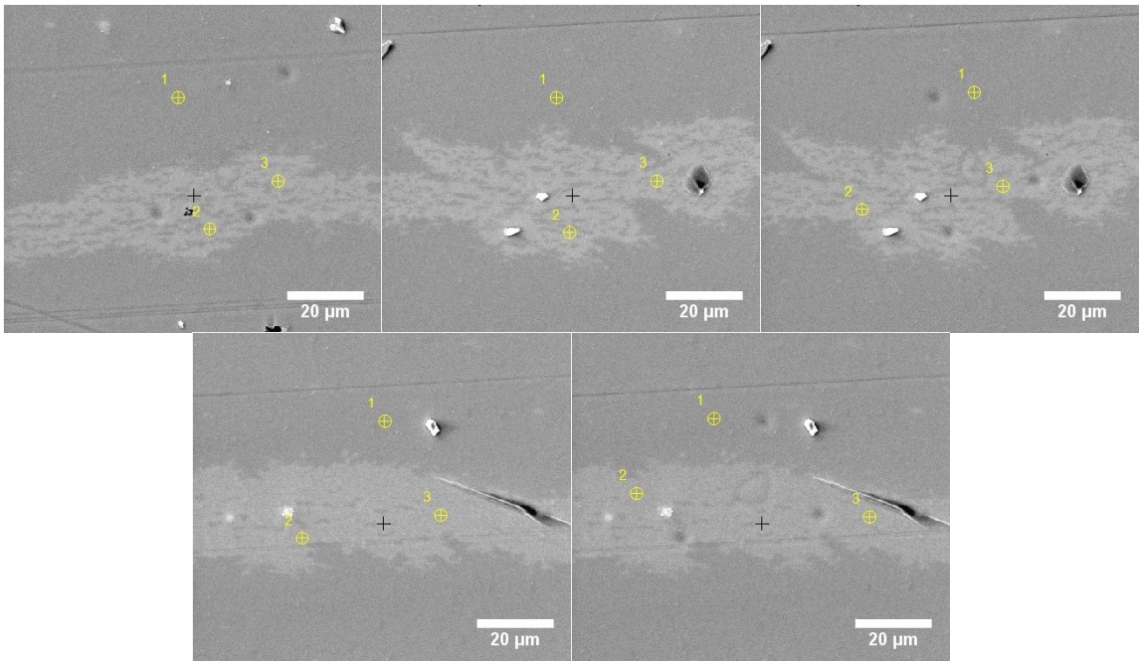

Fig. S10 SEM image of the PPDT2FBT:$PC_{61}BM$ surface after 6 months at 85 °C with marked 0.65 µm diameter spot locations of Auger spectroscopy was measured. Position 1 is the surface of the BHJ, while position 2 & 3 is the spot scan location of the flat surface feature.

S.9. Auger electron spectra of surface features present on thermally aged PPDT2FBT:$PC_{61}BM$ BHJ

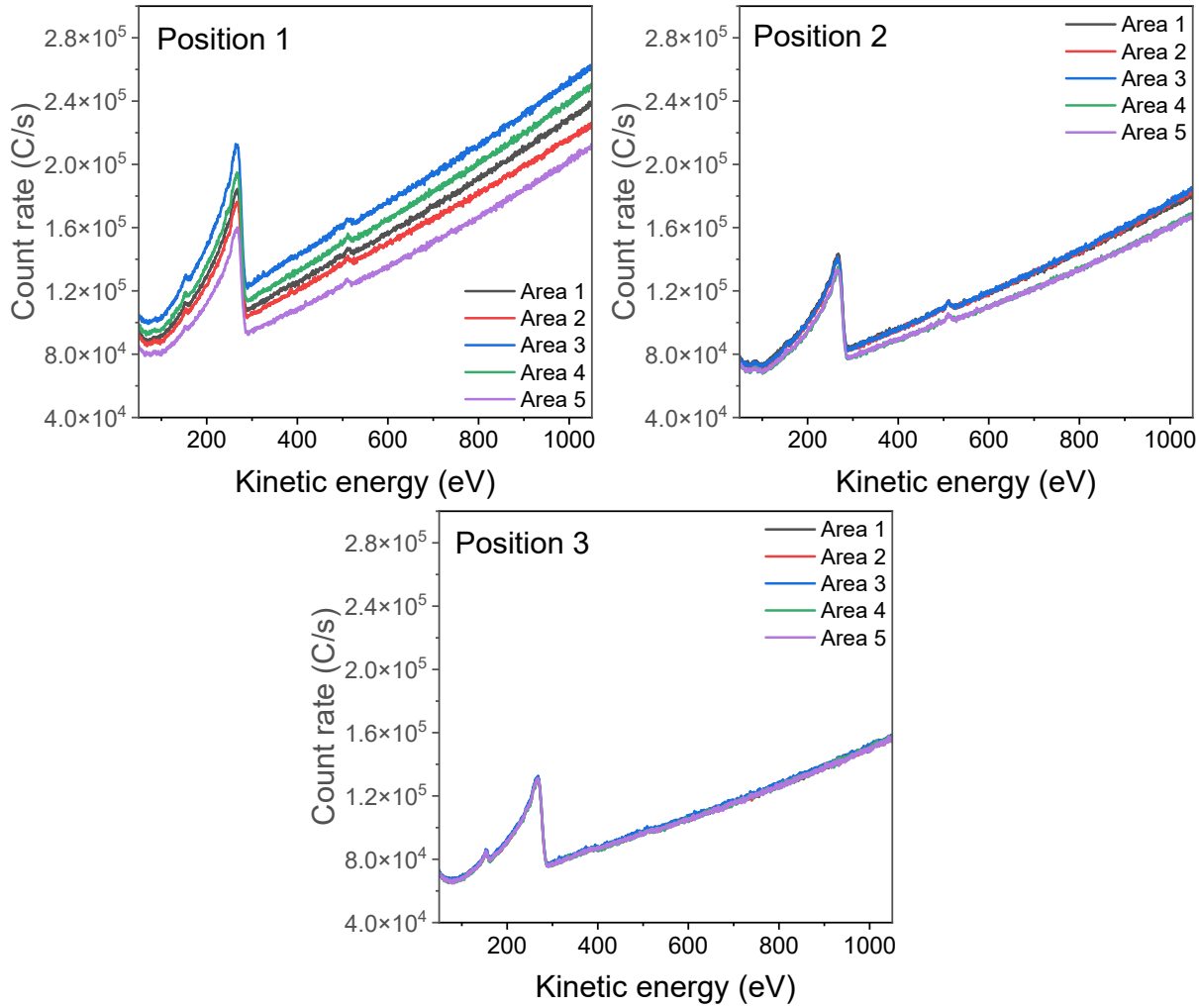

Fig. S11 AES of PPDT2FBT:$PC_{61}BM$ surface after 8 hours at 120 °C with marked locations of Auger spectroscopy was measured. Position 1 & 2 is the spot scan location over the short and long crystals, respectively, while position 3 is over the surface of the BHJ. Position locations can be seen in Fig. S9.

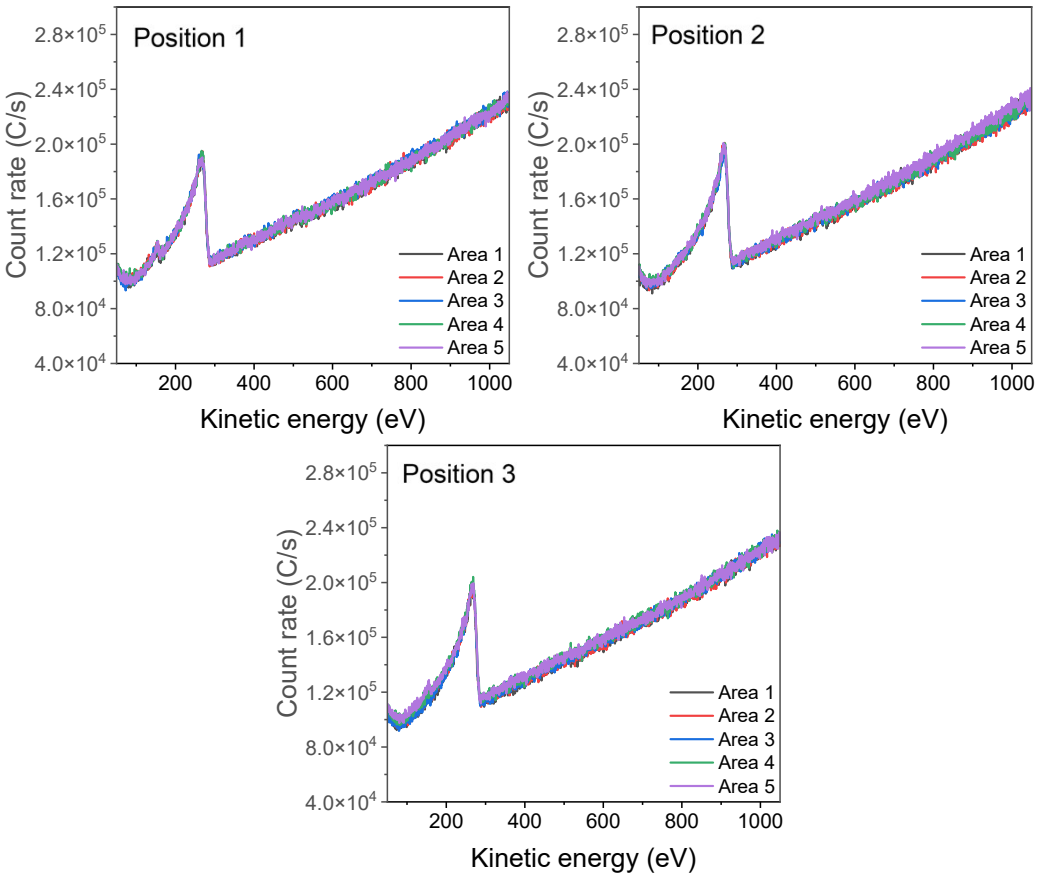

Fig. S12 AES of PPDT2FBT:$PC_{61}BM$ surface after 8 hours at 120 °C with marked locations of Auger Spectroscopy was measured. Position 1 & 2 is the spot scan location over the short and long crystals, respectively, while position 3 is over the surface of the BHJ. Position locations can be seen in Figure S10.

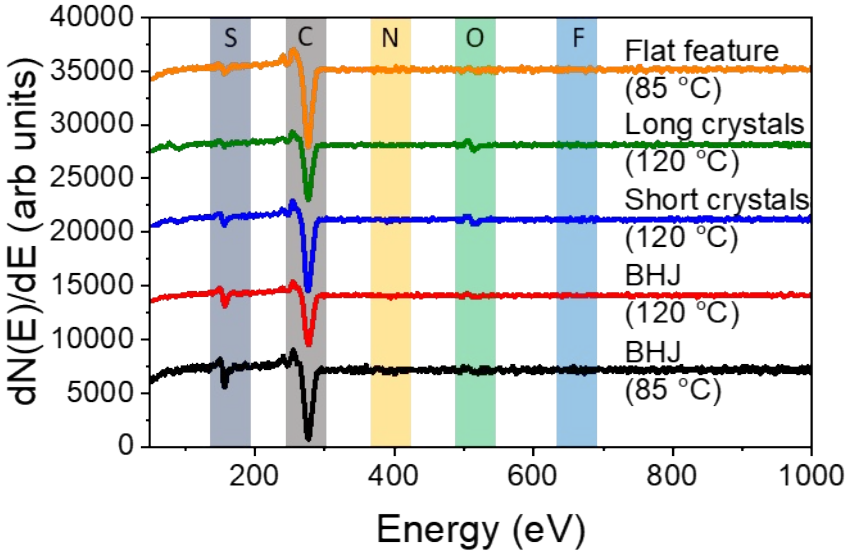

Fig. S13 Smoothed and derived Auger spectra of specific features found on the surface of PPDT2FBT:PC61BM annealed at either 85 °C or 120 °C. Highlighted are the predicted peak positions of elements suspected to be present at the surface. The spectra are an average of 5 different scanning locations.

S.10. Neutral impact collision ion scattering spectra of bulk heterojunction

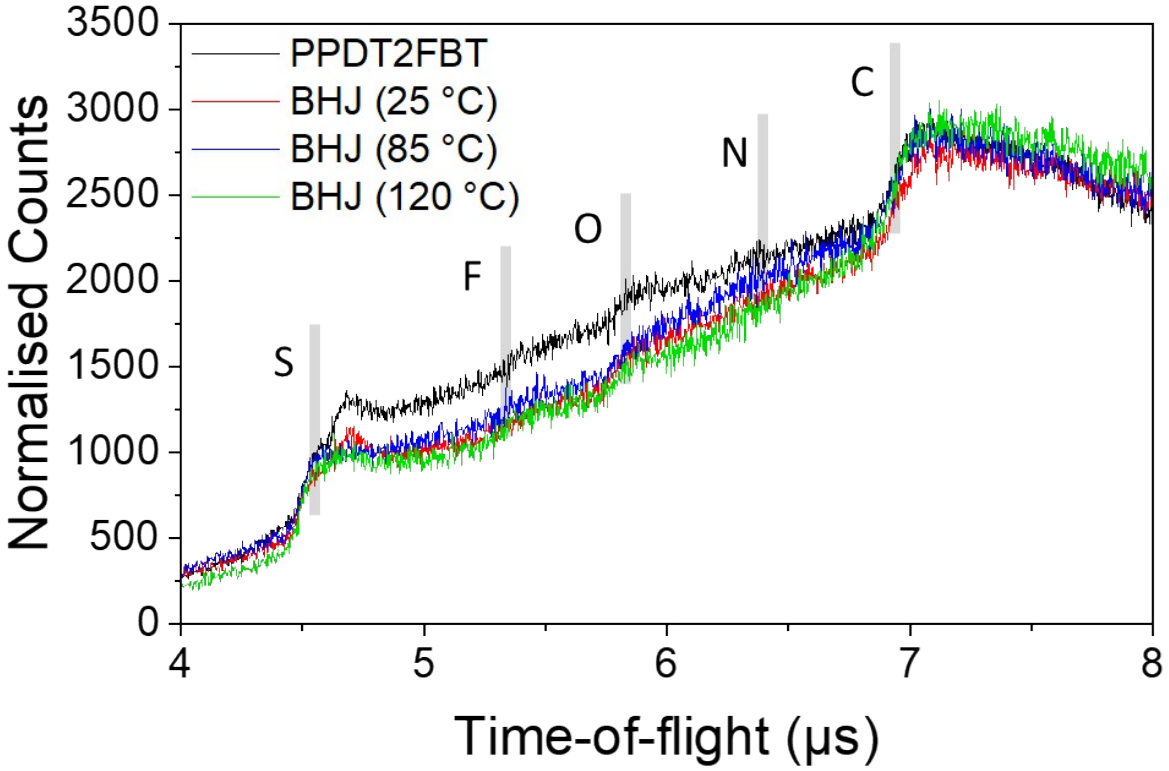

Fig. S14 NICISS ToF spectra of either pristine PPDT2FBT (black line) or PPDT2FBT:PC61BM BHJ (coloured lines). The BHJ is either non-annealed (25 °C) (red line), aged at 85 °C for 6 months (blue) or aged at 120 °C for 24 hours (green line). Counts are normalised based on carbon peak height. Spectra features due to sulphur, fluorine, oxygen, nitrogen, and carbon are marked with vertical bars.

S.10. Area occupied by surfaces of bulk heterojunction aged at 85 °C

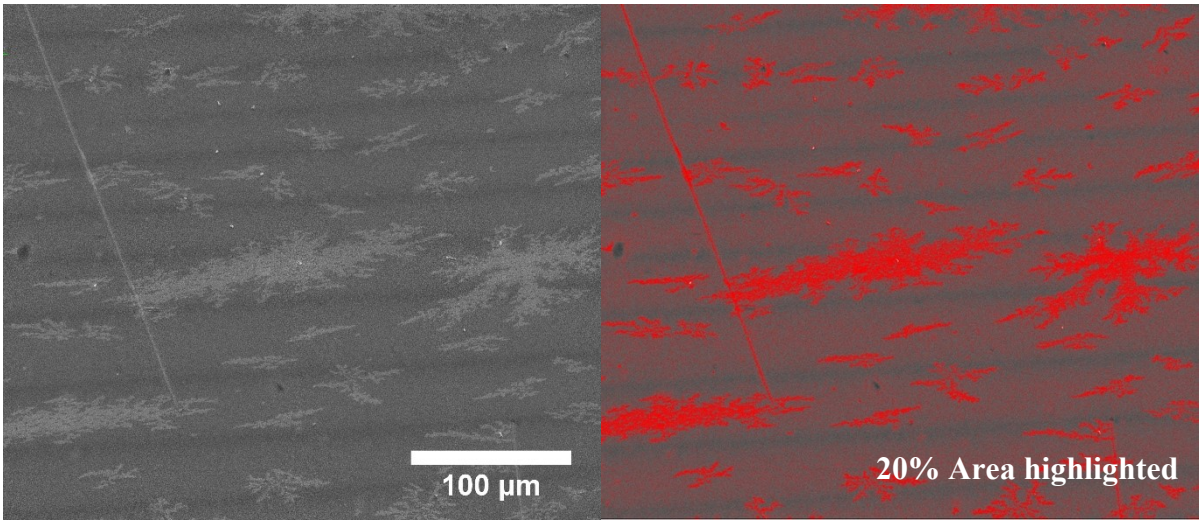

Fig. S15 SEM surface of PPDT2FBT:$PC_{61}BM$ active layer aged at 85 °C for 6 months (LEFT), with highlighted area used for determining area of flat fullerene features.

S.11. Dynamic mechanical thermal analysis of thermally aged PPDT2FBT:$PC_{61}BM$ blends

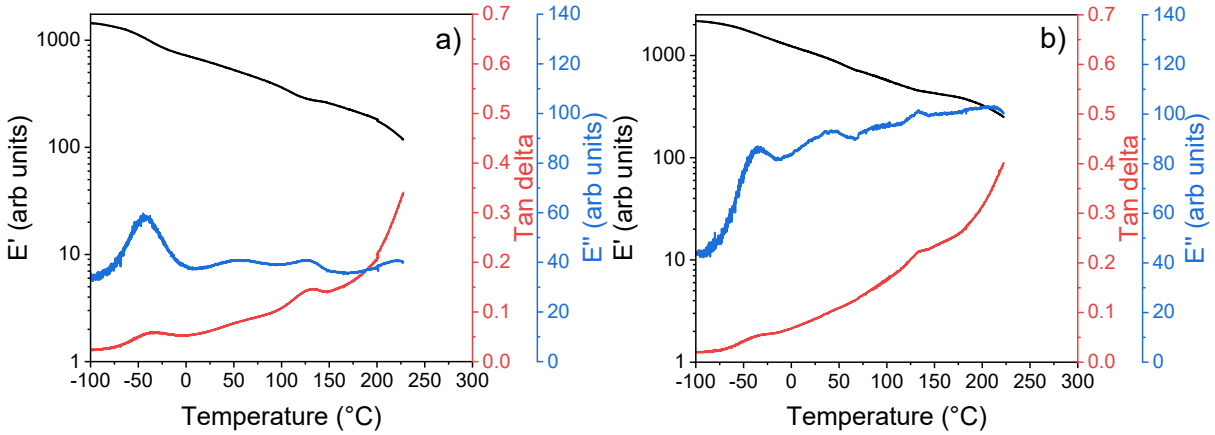

Fig. S16 DMTA of PPDT2FBT:$PC_{61}BM$ samples after thermal annealing: a) 85 °C for 30 minutes and b) 15 hours.

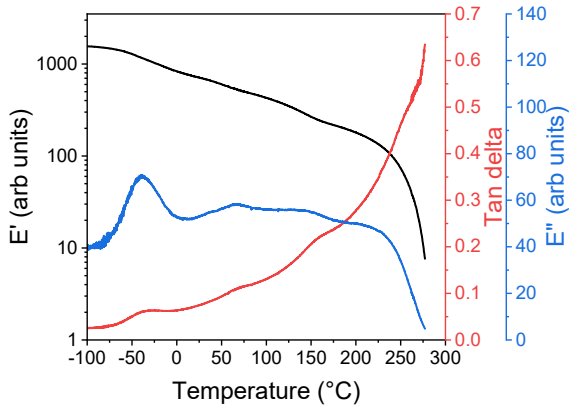

Fig. S17 DMTA of PPDT2FBT:$PC_{61}BM$ samples after thermal annealing at 120 °C for 15 hours.

S.12. References

1. F. C. Krebs, *Solar Energy Materials and Solar Cells*, 2008, **92**, 715-726.
2. F. C. Krebs, *Solar energy materials and solar cells*, 2009, **93**, 394-412.
3. R. Po, A. Bernardi, A. Calabrese, C. Carbonera, G. Corso and A. Pellegrino, *Energy & Environmental Science*, 2014, **7**, 925-943.
4. C. W. T. Bulle-Lieuwma, W. J. H. Van Gennip, J. K. J. Van Duren, P. Jonkheijm, R. A. J. Janssen and J. W. Niemantsverdriet, *Applied surface science*, 2003, **203**, 547-550.
5. F. Frigerio, M. Casalegno, C. Carbonera, T. Nicolini, S. V. Meille and G. Raos, *Journal of Materials Chemistry*, 2012, **22**, 5434-5443.